THE ASTROPHYSICAL JOURNAL, 500:L13–L16, 1998 June 10

FAR-ULTRAVIOLET OBSERVATIONS OF NGC 4151 DURING THE *ORFEUS-SPAS II* MISSION

B. R. ESPEY,[1] G. A. KRISS,[1] J. H. KROLIK,[1] W. ZHENG,[1] Z. TSVETANOV,[1] AND A. F. DAVIDSEN[1]
Center for Astrophysical Sciences, Department of Physics and Astronomy, Johns Hopkins University, Charles and 34th Street, Bloomberg Center, Baltimore, MD 21218; espey@pha.jhu.edu, gak@pha.jhu.edu, jhk@pha.jhu.edu, zheng@pha.jhu.edu, zlatan@pha.jhu.edu, afd@pha.jhu.edu
Received 1997 November 14; accepted 1998 April 10; published 1998 June 1

ABSTRACT

We observed the Seyfert 1 galaxy NGC 4151 on 11 occasions at 1–2 day intervals using the Berkeley spectrometer during the *ORFEUS-SPAS II* mission in 1996 November. The mean spectrum covers 912–1220 Å at ~0.3 Å resolution with a total exposure of 15,658 s. The mean flux at 1000 Å was 4.7×10^{-13} ergs cm^{-2} s^{-1} Å^{-1}. We identify the neutral hydrogen absorption with a number of components that correspond to the velocity distribution of H I seen in our own Galaxy as well as features identified in the C IV λ1549 absorption profile by Weymann et al. The main component of neutral hydrogen in NGC 4151 has a total column density of log $N_{\rm H\,I} = 18.7 \pm 1.5$ cm^{-2} for a Doppler parameter $b = 250 \pm 50$ km s^{-1}, and it covers 84% ± 6% of the source. This is consistent with previous results obtained with the Hopkins Ultraviolet Telescope. Other intrinsic far-UV absorption features are not resolved, but the C III* λ1176 absorption line has a significantly higher blueshift relative to NGC 4151 than the C III λ977 resonance line. This implies that the highest velocity region of the outflowing gas has the highest density. Variations in the equivalent width of the C III* λ1176 absorption line anticorrelate with continuum variations on timescales of days. For an ionization timescale of less than 1 day, we set an upper limit of 25 pc on the distance of the absorbing gas from the central source. The O VI λ1034 and He II λ1085 emission lines also vary on timescales of 1–2 days, but their response to the continuum variations is complex. For some continuum variations they show no response, while for others the response is instantaneous to the limit of our sampling interval.

Subject headings: galaxies: active — galaxies: individual (NGC 4151) — galaxies: nuclei — galaxies: Seyfert — ultraviolet: galaxies

1. INTRODUCTION

The Seyfert 1 galaxy NGC 4151 has been a favorite of observers wishing to use variability as a probe of the inner workings of active galactic nuclei. NGC 4151's ultraviolet variability was first noted in a rocket flight (Hartig 1979). Numerous campaigns using the *International Ultraviolet Explorer* (*IUE*) have since monitored the continuum, emission lines, and absorption lines (Ulrich et al. 1984; Bromage et al. 1985; Clavel et al. 1992; Crenshaw et al. 1996; Edelson et al. 1996). A tendency for the equivalent widths of the high-ionization lines (e.g., C IV) to correlate directly with variations in the continuum while low-ionization lines such as C II were anticorrelated has been noted in *IUE* studies of the absorption lines (Bromage et al. 1985). In contrast, monitoring of the C IV absorption line a decade later using the Goddard High-Resolution Spectrograph (GHRS) on the *Hubble Space Telescope* at moderate spectral resolution ($R \sim 15{,}000$) showed no variation in strength or shape over a baseline of several years (Weymann et al. 1997).

Significant UV continuum and emission-line variability on timescales as short as 1–2 days were seen in the continuous monitoring of NGC 4151 with *IUE* in 1994 December (Crenshaw et al. 1996). Monitoring with the Hopkins Ultraviolet Telescope (HUT) during the Astro-2 mission over the 912–1820 Å band at ~2 day intervals showed no change in the C IV equivalent width but revealed substantial variations in the H I column and in low-ionization ions such as C III and Si IV that were correlated with variations in the continuum (Kriss et al. 1996, 1998). With the low-resolution ($R \sim 300$) HUT data, however, we could not identify which of the several components in the complex C IV absorption profile was associated with these variations.

The HUT Astro-1 and Astro-2 observations of NGC 4151 revealed numerous absorption lines over a wide range of ionization states in the 912–1200 Å band (Kriss et al. 1992, 1995). Our observations with the Berkeley spectrometer on *ORFEUS-SPAS II* were intended to make use of its higher resolution ($R \sim 3300$) relative to HUT in order to study the structure and time response of the absorption-line systems in greater detail. We present here the mean spectrum and key features of the variability we saw during the *Orbiting and Retrievable Far and Extreme Ultraviolet Spectrometers* (*ORFEUS*)–*Shuttle Pallet Satellite* (*SPAS*) *II* mission. Full details of the individual observations will be described in a subsequent publication.

2. OBSERVATIONS AND DATA REDUCTION

We obtained spectra of NGC 4151 at 11 epochs with the Berkeley spectrograph during the *ORFEUS-SPAS II* mission in 1996 November/December. Exposure times ranged from 600 to 2200 s, with a total exposure of 15,658 s. The general design of the Berkeley spectrograph is discussed by Hurwitz & Bowyer (1986, 1996), while the calibration and the performance of the *ORFEUS-SPAS II* mission are described by Hurwitz et al. (1998b).

The Berkeley spectrometer has a two-dimensional detector, so the NGC 4151 data were obtained through a 26″ diameter aperture simultaneously with airglow spectra through a larger aperture offset by 2′.4. The signal-to-noise ratio varies greatly with wavelength, and it is highest near the O VI and Lyα emission lines. Due to a reflection in the Berkeley spectrometer, undispersed Lyα airglow produces a rapid increase in the background level below ~950 Å. Correction for this and other instrumental features is discussed in Hurwitz et al. (1998b), and

[1] *ORFEUS-SPAS II* Guest Investigator.

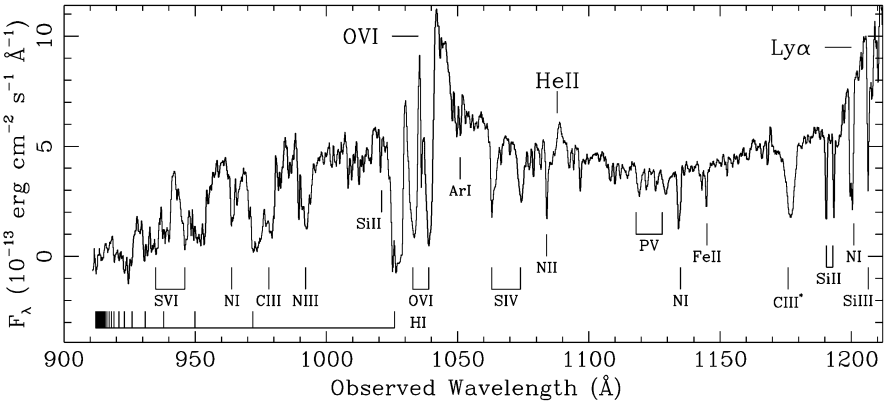

FIG. 1.—Observed mean airglow-subtracted spectrum of NGC 4151 obtained with the Berkeley spectrometer on the *ORFEUS-SPAS II* mission in 1996 November/December.

our data were extracted and calibrated using the prescription recommended by the Berkeley spectrometer team.

To maximize the signal-to-noise ratio (S/N), we binned these basic spectra into larger wavelength bins of 0.15 Å, roughly half of a resolution element (Hurwitz et al. 1998b). To correct the wavelength scale for slight inaccuracies in telescope pointing, we shifted the object spectra to place the Galactic Si II λλ1190 and 1193 absorption features at a heliocentric velocity of 60 km s^{-1} (the Galactic H I velocity determined by Murphy 1998). From a comparison among all the observed Galactic absorption features in the spectrum, we estimate that our wavelength scale is accurate to 40 km s^{-1} (1 σ).

The contemporaneous airglow spectra were extracted in exactly the same manner as the target data. Airglow emission lines were fitted using Gaussian components. A comparison of the line widths of isolated emission lines through both the airglow aperture and the smaller target aperture provided the correction factor needed to generate a model airglow spectrum tailored to each target spectrum. Our template airglow spectra were then corrected for slight wavelength offsets and scaled to match the flux observed through the target aperture by linear shifting and by scaling to the Lyβ line in the object spectrum. The mean airglow-subtracted, exposure-weighted spectrum is shown in Figure 1.

TABLE 1

ABSORPTION LINES IN THE MEAN SPECTRUM OF NGC 4151

Line	EW (Å)	$v_\odot$[a] (km s^{-1})	FWHM (km s^{-1})	Origin[b]
S VI λ933.38	3.96 ± 1.14	533	567 ± 131	N
S VI λ944.52	3.60 ± 1.00	533	567 ± 131	N
N I λ963.99	0.55 ± 0.26	533	567 ± 131	N
C III λ977.02	3.69 ± 1.32	508	567 ± 110	N
N III λ990.79	2.54 ± 0.09	499	1000 ± 200	N
Si II λ1020.70	0.26 ± 0.03	10	142 ± 23	G
O VI λ1031.93	3.54 ± 0.28	455	...	N
O VI λ1037.62	3.81 ± 0.47	455	...	N
Ar I λ1048.22	0.31 ± 0.10	838	277 ± 120	N
S IV λ1062.67	1.49 ± 0.09	379	768 ± 50	N
S IV λ1073.28	1.28 ± 0.09	379	768 ± 50	N
N II λ1083.99	0.46 ± 0.04	46	146 ± 15	N
P V λ1117.98	0.60 ± 0.21	377	468 ± 140	N
P V λ1128.01	0.64 ± 0.34	377	468 ± 140	N
Fe II λ1144.94	0.40 ± 0.06	18	158 ± 28	G
C III* λ1175.70	2.32 ± 0.12	341	846 ± 53	N
Si II λ1190.42	0.58 ± 0.03	60	154 ± 10	G
Si II λ1193.29	0.58 ± 0.03	60	154 ± 10	G
N I λ1199.9	1.31 ± 0.08	103	393 ± 29	G
Si III λ1206.50	0.52 ± 0.04	33	140 ± 12	G

[a] The Galactic Si II λ1190 and λ1193 lines (with $v_\odot$ = 60 km s^{-1}) were used to align the wavelength scale. Velocities are accurate to ~40 km s^{-1} (1 σ).

[b] N = lines intrinsic to NGC 4151; G = Galactic absorption lines.

The mean spectrum shows that NGC 4151 had an intensity intermediate between the observations made during the Astro-1 and Astro-2 missions. We use the mean spectrum to determine the basic parameters of both continuum and line components (see Tables 1 and 2). These and subsequent fits were performed using χ^2 minimization in the spectral fitting program SPECFIT (Kriss 1994). We model the continuum as a power law in f_λ. We correct for foreground extinction by using a Cardelli, Clayton, & Mathis (1989) curve assuming $E(B-V) = 0.04$ (Kriss et al. 1995) and $R_V = 3.1$.

The best-fit, extinction-corrected continuum is $f_\lambda = 8.20 \times 10^{-13}(\lambda/1000)^{-1.37}$. For the Ly$\alpha$, He II λ1085, and O VI λ1036 emission lines, we assume the shape found by Kriss et al. (1992). Absorption features were modeled using components that are Gaussians in either equivalent width or optical depth. The features identified in the mean spectrum and their parameters are listed in Table 1. We find no evidence for a change in power-law index among the individual observations. To fit the variations in the individual emission and absorption lines, we fix the wavelength and line width of each component and fit the intensity or equivalent width in every individual exposure.

3. ABSORPTION FEATURES AND THEIR VARIABILITY

3.1. *Neutral Hydrogen Absorption*

Measuring the intrinsic neutral hydrogen column in NGC 4151 requires a good S/N in the high-order Lyman lines since the low-order lines are heavily saturated. An S/N of ~5 per bin at the Lyman limit required further binning of the mean spectrum to 0.6 Å pixel^{-1}. This is still far better than the ~3 Å resolution of HUT. Unfortunately, the high background noise at short wavelengths prevents a good measure of the hydrogen column in the individual observations. No significant variations in the strong Lyα and Lyβ absorption lines are seen, presumably because of their high optical depth. The higher spectral resolution of the Berkeley spectrometer compared with HUT, however, enables us to deblend the hydrogen absorption in the mean spectrum and to separate the complex assortment of Galactic and intrinsic components that are present.

The outflowing H I absorption in NGC 4151 brackets strong

TABLE 2
H I Absorption in NGC 4151

Component	$v_\odot$ (km s^{-1})	log N(H I) (cm^{-2})	b (km s^{-1})	Covering Fraction
NGC 4151 A	−540	15.5 ± 0.1	45 ± 0	0.95 ± 0.24
Galactic	60	20.3 ± 0	75 ± 0	1.00 ± 0
NGC 4151 C + D + E	451	18.70 ± 1.5	250 ± 50	0.84 ± 0.06
NGC 4151 F	982	19.61 ± 0.5	45 ± 0	0.73 ± 0.80

absorption by neutral hydrogen in our own Galaxy. Galactic H I 21 cm emission observed toward NGC 4151 shows multiple components with a total column density of $\sim 2 \times 10^{20}$ cm^{-2} at a mean heliocentric velocity of 60 km s^{-1} (Murphy et al. 1996; Murphy 1998). This complex structure is reflected in our *ORFEUS-SPAS II* data by the large line widths observed for Galactic absorption features.

To model the Galactic H I absorption, we first fitted the absorbing column, location, and line width of the four main components in Murphy's 21 cm profile. We then generated an H I absorption-line template smoothed to the resolution of our spectrum. We find that although the total absorbing column is 2×10^{20} cm^{-2} and the separation of the components is less than our instrumental resolution, the resulting absorption-line profile is optically thick but not black, which is consistent with our observations of the high-order Lyman lines.

We similarly determined the location and line width of two narrow, low-ionization components seen in GHRS spectra (components A and F), which are identified with outflowing and halo material in NGC 4151, respectively (Weymann et al. 1997). We fitted these components in the mean spectrum and included a broad component to represent higher ionization material (an unresolved blend of components C, D, and E). These several components and their best-fit parameters are summarized in Table 2. The reduced χ^2 of the fit is quite large (187.6), but this is largely because of an underestimate of the true errors in the binned data. Near O VI in the rebinned spectrum, the formal S/N based on photon statistics is ~85, but the flat field is only accurate to ~5%.

Our best fit to the broad absorption gives log ($N_{\rm H\,I}$) = 19.7 and b = 250 km s^{-1}, covering ~84% of the source. This broad component is consistent with that seen in the HUT Astro-1 and Astro-2 spectra (Kriss et al. 1992, 1995). It has a width and partial covering similar to that seen during Astro-2 and a total column intermediate between the Astro-1 and Astro-2 values, consistent with the intermediate value of the continuum flux seen in these new observations. Component F, at the systemic velocity of NGC 4151 and probably associated with its interstellar medium or halo, has a column density an order of magnitude lower than the optically thick component suggested by Kriss et al. (1995), but it is still optically thick. Given the lack of broad, black Mg II absorption at this velocity in the GHRS spectrum (Weymann et al. 1997), it is likely that the actual column density is at the lower end of the range permitted by our errors.

3.2. *Other Absorption Features*

Correcting for the 90 km s^{-1} resolution of the Berkeley spectrometer, the unresolved Galactic absorption features have FWHM ~ 100 km s^{-1} (see Table 1). This is roughly what is expected from the 21 cm H I profile toward NGC 4151 (Murphy 1998), and it is consistent with Galactic lines in the GHRS spectra. Our identified Galactic absorption lines are similar to those reported for the 3C 273 sight line by Hurwitz et al. (1998a).

Accurate measurements of O VI absorption intrinsic to NGC 4151 proved difficult because of the overlapping absorption and emission features. What is apparent, however, is that the dominant absorption in the O VI doublet is similar to the absorption features seen in the C IV line (Weymann et al. 1997; Hutchings et al. 1998). It is optically thick, but the broad width (~1100 km s^{-1}) and the nonblack line centers imply partial covering. We see no significant variations in the O VI absorption equivalent width. More detailed analysis of the O VI troughs will be reported in a future publication.

As described by Bromage et al. (1985) and Kriss et al. (1992), C III* λ1176 can be used together with C III λ977 to measure the density of the absorbing gas. In the Astro-1 and Astro-2 HUT data, both lines were assumed to arise in the same absorbing region. The higher resolution *ORFEUS-SPAS II* data shows that the situation is not so simple—the mean velocity of the C III* λ1176 absorption is significantly higher than that of C III λ977. C III λ977 is less blueshifted, and it has a velocity comparable to that of component D in the C IV profile of Weymann et al. (1997). C III* λ1176 is closer in velocity to component C, but the 850 km s^{-1} width of the feature gives considerable overlap to all broad C IV components C, D, and E. If the gas outflowing from NGC 4151 is accelerating, this places the highest density gas in the outflow farthest from the source.

In contrast to the results for Lyβ and O VI absorption, we detect strong variations in the C III* λ1176 and S IV λ1073 absorption lines. (S IV λ1062 is blended with Galactic absorption.) The constancy of the Galactic features throughout the mission confirms the reality of these variations. As shown in Figure 2, both C III* and S IV anticorrelate with the observed continuum variations. To within the 1–2 day sampling of our measurements, the continuum and line variations are instantaneous, with no significant lag.

Following the formalism of Krolik & Kriss (1997), we can use the ionization and recombination timescales to set limits on the location of the absorbing material. For an observed ionization timescale $t_{\rm ion}$, an ionizing flux density at the Earth $f_{\rm ion}$, a mean photoionization cross section $\langle\sigma_{\rm ion}\rangle$, a threshold ionization energy $h\nu_T$, and a distance to the source D (15 Mpc for NGC 4151), they find that the material must lie at a radius

$$r \leq \left(\frac{f_{\rm ion} \langle \sigma_{\rm ion} \rangle t_{\rm ion}}{h\nu_T} \right)^{1/2} D. \quad (1)$$

The decrease in the C III* λ1176 equivalent width during the increase in the continuum flux observed from day 334 to 335 implies that ionization is dominant in this interval. We thus have an upper limit of 1 day on $t_{\rm ion}$. Using a photoionization cross section of $\langle\sigma_{\rm ion}\rangle = 1.6 \times 10^{-18}$ cm^2 (Osterbrock 1989, p. 36) at the ionization threshold for C III* (41.4 eV, or 300

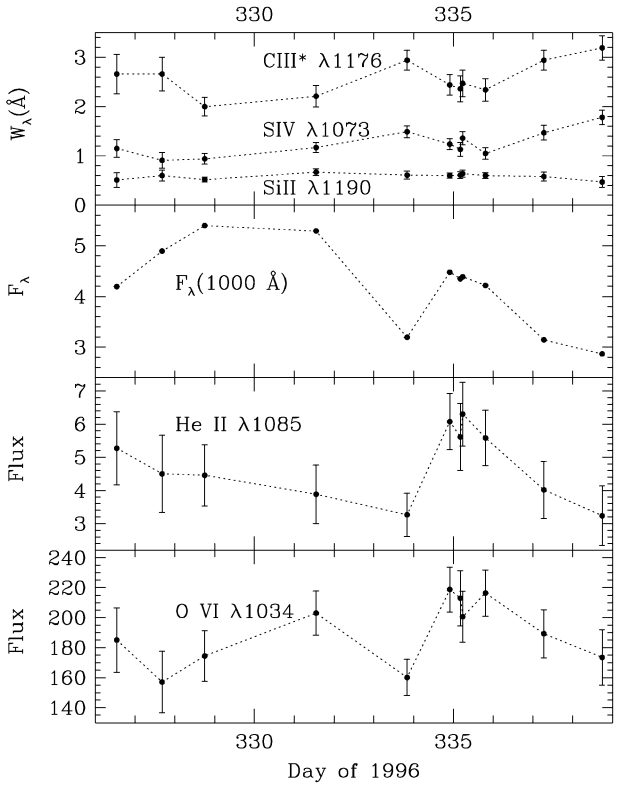

FIG. 2.—Absorption-line, continuum, and emission-line variations with time for the 11 observations of NGC 4151 during the *ORFEUS-SPAS II* mission. Note that the Galactic Si II λ1190 equivalent width in the top panel shows no evidence of variation. The continuum flux at 1000 Å is in units of 10^{-13} ergs cm^{-2} s^{-1} Å^{-1}. The He II λ1085 and O VI λ1034 emission-line fluxes are in units of 10^{-13} ergs cm^{-2} s^{-1}.

Å), and extrapolating our best-fit, extinction-corrected continuum to 300 Å, we find $r < 25$ pc. This is comparable to the limit found using the variation in the H I column seen during the HUT Astro-2 observations of NGC 4151 (Krolik & Kriss 1997; Kriss et al. 1998).

4. EMISSION FEATURES

The dominant emission features in our data are O VI λ1034, He II λ1085, and the blue wing of Lyα. The partial Lyα line and the strength of the Lyα airglow preclude any meaningful determination of the intrinsic line strength. Variations in the O VI and He II fluxes compared with the continuum are shown in Figure 2. The fractional variation in the He II flux ($F_{\rm var}$ = 0.23) is comparable to that in the continuum flux [$F_{\rm var}(1000) = 0.20$]. In contrast, the variation seen in the O VI emission is much less: $F_{\rm var} = 0.12$. Our data set is not large enough to compute meaningful cross-correlation functions, but qualitatively one can see that there is a significant response in the emission lines on timescales of 2 days or less. The detailed response, however, is not the typical smeared and delayed variation seen in prior monitoring campaigns. While the continuum is rising in the first three observations, O VI and He II are constant or falling in flux. In contrast, both lines track well the dip and subsequent rise in the continuum flux at days 334 to 336.

We thank the Berkeley spectrometer science team and all those whose participation helped make the *ORFEUS-SPAS II* mission such a success. This work was supported by NASA LTSA grant NAG 5-3255 to the Johns Hopkins University.

REFERENCES

Bromage, G., et al. 1985, MNRAS, 215, 1
Cardelli, J. A., Clayton, G. C., & Mathis, J. S. 1989, ApJ, 345, 245
Clavel, J., et al. 1992, ApJ, 393, 113
Crenshaw, D. M., et al. 1996, ApJ, 470, 322
Edelson, R. A., et al. 1996, ApJ, 470, 364
Hartig, G. R., Jr. 1979, Ph.D. thesis, Johns Hopkins Univ.
Hurwitz, M., et al. 1998a, ApJ, 500, L61
———. 1998b, ApJ, 500, L1
Hurwitz, M., & Bowyer, S. 1986, Proc. SPIE, 627, 375
———. 1996, in Astrophysics in the Extreme Ultraviolet, ed. S. Bowyer & R. F. Malina (Dordrecht: Kluwer), 601
Hutchings, J. B., et al. 1998, ApJ, 492, L115
Kriss, G. A. 1994, in ASP Conf. Ser. 61, Astronomical Data Analysis Software and Systems III, ed. D. R. Crabtree, R. J. Hanisch, & J. Barnes (San Francisco: ASP), 437
Kriss, G. A., Davidsen, A. F., Zheng, W., Kruk, J. W., & Espey, B. R. 1995, ApJ, 454, L7
Kriss, G. A., et al. 1992, ApJ, 392, 485
———. 1998, in preparation
Kriss, G., Krolik, J., Grimes, J., Tsvetanov, Z., Zheng, W., & Davidsen, A. 1996, in ASP Conf. Ser. 113, Emission Lines in Active Galaxies: New Methods and Techniques, (IAU Colloq. 159), ed. B. M. Peterson, F.-Z. Cheng, & A. S. Wilson (San Francisco: ASP), 453
Krolik, J. H., & Kriss, G. A. 1997, in ASP Conf. Ser. 128, Mass Ejection from Active Galactic Nuclei, ed. R. Weymann, N. Arav, & I. Shlossman (San Francisco: ASP), 132
Murphy, E. M. 1998, in preparation
Murphy, E. M., Lockman, F. J., Laor, A., & Elvis, M. 1996, ApJS, 105, 369
Osterbrock, D. E. 1989, Astrophysics of Gaseous Nebulae (Mill Valley: University Science Books)
Ulrich, M. H., et al. 1984, MNRAS, 206, 221
Weymann, R. J., Morris, S. L., Gray, M. E., & Hutchings, J. B. 1997, ApJ, 483, 717